

Eco Friendly Synthesis and Structural Analysis of Ag₂O/Ag Nanoparticles Derived from Hibiscus Sabdariffa Extract

Ali K. Hattab

Department of Physics, College of Science, University of Wasit, Wasit

General Background: Nanotechnology enables the fabrication of novel materials with unique structural and optical properties, with silver oxide (Ag₂O) nanoparticles being of particular interest for catalytic, sensing, and optoelectronic applications. **Specific Background:** Conventional chemical synthesis of Ag₂O nanoparticles often involves toxic reagents and harsh conditions, posing environmental and biomedical limitations. **Knowledge Gap:** Despite advances in green chemistry, efficient, eco-friendly routes to control particle size, morphology, and stability of Ag₂O/Ag nanoparticles remain underexplored. **Aims:** This study develops an environmentally sustainable synthesis of Ag₂O/Ag nanoparticles using *Hibiscus sabdariffa* extract as a natural reducing and stabilizing agent. **Results:** X-ray diffraction confirmed a cubic crystal structure with an average crystallite size of 35.60 nm, while FESEM revealed irregular spherical particles averaging 57.2 nm. Energy-dispersive X-ray spectroscopy verified silver and oxygen elements, UV-Vis spectroscopy showed a 414 nm absorption peak with a 2.88 eV direct bandgap, and FTIR detected characteristic O-H, C-H, and Ag-O bonds. **Novelty:** This work demonstrates a cost-effective, plant-extract-based synthesis achieving precise structural and optical control without hazardous chemicals. **Implications:** The eco-friendly route supports scalable production of Ag₂O/Ag nanoparticles for applications in catalysis, biomedical devices, and optoelectronics, contributing to sustainable nanotechnology.

Highlights:

- Plant extract acts as natural reducing and stabilizing agent.
- Nanoparticles show 2.88 eV direct bandgap with 414 nm absorption.
- Sustainable method enables scalable, non-toxic production.

Keywords: Crystal, Silver, Spectrum, Nanoparticles, Bandgap

Introduction

Nanotechnology exists as a revolutionary science discipline between materials and engineering which enables the creation of materials with novel properties and functions. Metal oxide nanoparticles draw extensive scientific interest due to their distinct physical, chemical, and optical behavioral aspects which differ markedly from their bulk counterparts. The research community shows intense interest in silver oxide (Ag_2O) nanoparticles because of their uses in catalytic reactions as well as sensors and antimicrobial and optoelectronic device applications [1]. The traditional production methods of Ag_2O nanoparticles require chemical reduction with dangerous stabilizing agents and reducing agents resulting in hazardous environmental impact and health risks. The traditional manufacturing methods yield toxic waste products while needing forceful reaction parameters that restrict large-scale manufacturing. Surface contamination with toxic chemical residues acts as a constraint to applying Ag_2O nanoparticles in biomedical and environmental work. Researchers now turn to investigating different eco-friendly synthesis approaches because of these drawbacks [2]. Plant extract-based synthesis methods now represent a successful replacement for traditional chemical production techniques. The method complies with fundamental principles of green chemistry through its use of sustainable resources along with its reduction of dangerous substances. Nanoparticles produced through plant extract synthesis benefit from stabilizing properties and reducing capabilities due to their biomolecule content which includes proteins and polyphenols flavonoids and terpenoids [3]. The natural compounds function to reduce metal ions and simultaneously protect the formed nanoparticles by creating surface alignment structures. The natural resource *Hibiscus sabdariffa* or roselle attracts interest as a biological agent for nanoparticle synthesis because it contains multiple phytochemicals [4]. The plant calyces show high concentrations of organic acids and anthocyanins together with polyphenols and other bioactive compounds which help reduce metal ions while stabilizing nanoparticles. The utilization of *Hibiscus sabdariffa* extract results in several beneficial aspects including cheap production conditions combined with low chemical consumption potential and the manufacturing of biologic nanoparticles that work with different usage areas [5]. Controlling particle size along with morphology and composition properties during green synthesis of Ag_2O /Ag nanoparticles proves difficult because these factors deeply affect their behavioral characteristics as well as their acceptable applications. The synthesis of Ag_2O /Ag nanoparticles requires a thorough examination of external variables including precursor concentration, pH value, temperature control, and reaction duration to reach optimal nanoparticle specifications [6]. Scientists need to study the relationships between plant biomolecules and metal ions throughout the synthesis process to gain an understanding of how nanoparticles develop and remain stable [7]. Scientists developed a sustainable synthesis approach for Ag_2O /Ag nanoparticles based on *Hibiscus sabdariffa* extract that works as a reducing and stabilization agent. An environmentally friendly synthesis approach will be developed through this study to produce nanoparticles along with efficient control over size and morphology [8]. Multiple investigation methods consisting of X-ray diffraction (XRD) together with field emission scanning electron microscopy (FESEM) and energy-dispersive X-ray spectroscopy (EDX) and UV-visible spectroscopy and Fourier transform infrared spectroscopy (FTIR) are used for evaluating structural and morphological and optical and surface properties of synthesized nanoparticles [9]. The research brings value to green nanotechnology by presenting an environmentally safe approach for synthesizing metal oxide nanoparticles that show promise in improving numerous technological applications [10].

Materials and Methods

A. Materials

The precursors used for the synthesis of Ag_2O /Ag nanoparticles included silver (I) nitrate AgNO_3 where the minimum assay of Ag is 99.8% with maximum limits of impurities of Cu below 2.0 ppm, SO_4 below 20.0 ppm, Fe below 2.0 ppm, Cl below 10 ppm, and Pb 2.0 ppm from Daejung, Korea. *Hibiscus sabdariffa* extract was obtained from dried calyces of the plant.

B. Methods

Preparation of Plant Extract: *Hibiscus sabdariffa* extract was obtained from dried calyces of the plant and evaluated in the dried form and ground into fine powder. From the powder, 1 gram was weighed and in a clean beaker, 2 grams of the powder was dissolved in 100 mL distilled water. The mixture was heated to 50°C for 1 hour with continuous stirring at 700 rpm to facilitate the extraction of *Hibiscus sabdariffa*. After heating, the mixture was cooled to room temperature and filtered using vacuum filtration and filter paper to remove residues. The

filtrate, which contains *Hibiscus sabdariffa* extract, was used in the synthesis approach as a natural reducing and stabilizing agent.

Green Synthesis of Ag₂O/Ag nanoparticles: silver (I) nitrate AgNO₃ dissolved in 100 ml distilled water at 25 °C under vigorous stirring at 700 rpm for 1h. to form two clear solutions, with one molar. Slowly add the *Hibiscus sabdariffa* extract to the solution while continuously stirring, allowing *Hibiscus sabdariffa* to act as a reducing and stabilizing agent for silver ions. Adjust the pH of the solution to an alkaline range (~12) by adding NaOH drop by drop, facilitating the precipitation of metal oxides. Stir the reaction mixture for 1h, maintaining the temperature at around 70-80°C. A color change into a dark brown hue solution indicates the formation of the Ag₂O/Ag nanoparticles. The precipitate was washed, dried at 100°C for 4 hours, and calcined at 400°C for 2 hours.

C. Characterization Techniques

Different techniques were used to analyze the synthesized nanocomposites. The X-ray Diffraction (XRD) analysis was conducted using a PANalytical X'Pert PRO diffractometer equipped with Cu K α radiation ($\lambda = 1.54060 \text{ \AA}$), operated at 40 kV and 30 mA. The diffractogram was recorded in the 2θ range from 10° to 80° with a step size of 0.02° at a scanning rate of $1^\circ/\text{min}$. Fourier Transform Infrared (FT-IR) spectra were obtained using a Bruker Alpha II FT-IR spectrometer in the range of $(4000 \text{ to } 400) \text{ cm}^{-1}$ at a resolution of 4 cm^{-1} . The sample was mixed with potassium bromide (KBr) to form pellets for transmission measurements. The recorded spectra were analyzed to confirm the presence of characteristic bonds of Ag₂O/Ag, particularly the Ag -O stretching vibrations. The optical properties of the nanocomposites were studied using a Shimadzu UV-2600 UV-Vis spectrophotometer. The absorption spectrum was measured in the wavelength range of 200 to 800 nm. The sample was dispersed in ethanol, and the absorbance was recorded. The optical band gap energy was calculated using the Tauc plot method by plotting $(\alpha h\nu)^2$ against photon energy ($h\nu$), where α is the absorption coefficient. The surface morphology and elemental composition of the synthesized nanocomposites were analyzed using a model TESCAN Mira3. The FESEM was operated at an accelerating voltage of 10 kV, and high-resolution images were captured at various magnifications to observe the particle size and distribution. For EDX analysis, the same device was used to perform elemental composition analysis at 20 kV to detect the presence of copper (Ag), and oxygen (O) in the sample. The elemental ratios of Ag were calculated to confirm the formation of the nanoparticles.

Results and Discussion

The X-ray diffraction (XRD) technique is employed to characterize the crystal structure of the prepared samples. Bragg's law Eq 1 can be applied to calculate the interplanar spacing (d) of lattice planes [11].

$$n\lambda = 2d \sin \theta \dots\dots\dots 1$$

Where n is the order of the diffraction peak, λ is the wavelength of incident X-rays, d is the interplanar spacing, and θ is the angle of incidence. This relationship is crucial for determining d in various crystal structures. The Debye-Scherrer Eq 2 was used to calculate the average crystallite size. It is employed to measure the size of crystal particle fragments.

$$D = (k\lambda)/(\beta \cos \theta) \dots\dots\dots 2$$

Where D is the crystallite size (nm), K is the crystallite's dimensionless form factor (0.94), X-ray wavelength ($\lambda = 0.154060 \text{ nm}$), θ is the Bragg diffraction angle (Radian), and β is the FWHM of the selected peak are all given (Radian) [12]. The X-ray diffraction (XRD) patterns of Ag₂O/Ag nanoparticles are shown in Fig. 1. The XRD patterns of Ag₂O/Ag nanoparticles identified a cubic crystal structure of Ag₂O according to the entry crystallography open database (COD) [96-431-8189] and a cubic crystal structure of Ag according to the entry cod [96-110-0137]. The three strongest peaks (2θ): 32.78° , 38.07° , and 54.87° correspond to planes and crystallite sizes of (111) plane:46.12 nm, (200) plane:29.73 nm, and (202) plane:30.96 nm, respectively. The average crystallite size is 35.60 nm. This result agrees with [13].

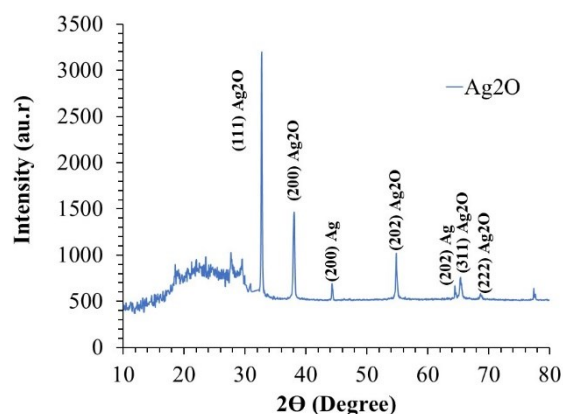
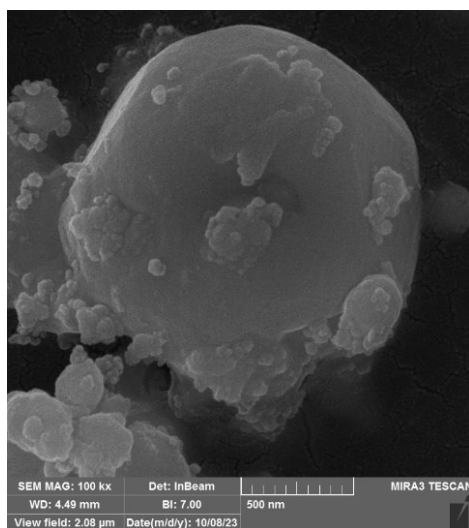
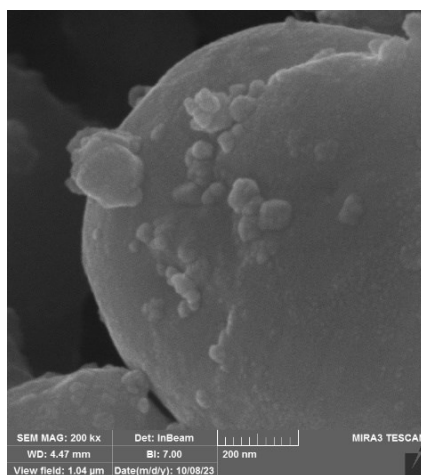


Figure 1. XRD pattern of Ag₂O/Ag nanoparticles.

The FESEM images in Fig. 2 (a-b) show the surface morphology of the Ag₂O/Ag nanoparticles. The FESEM images represent Ag₂O/Ag nanoparticles with irregular spherical shapes. The image at 200kx magnification displays enhanced surface details compared to 100kx magnification. Based on the provided scale bars the determined average particle size is approximately 57.2 nm.



(a)



(b)

Figure 2. FESEM images of Ag₂O/Ag nanoparticles (a) 100 kx and (b) 200 kx.

Fig. 3 a and b show the energy-dispersive X-ray (EDX) spectrum of Ag₂O/Ag nanoparticles. Also, give a quantitative result corresponding to silver and oxygen elements in a weight percentage (W%) and an atomic weight percentage (A%). The EDX spectrum of Ag₂O/Ag nanoparticles confirms several elemental compositions; Silver (Ag L α 1) at 3.01 KeV with 84.66 W%; 53.78 A%, Oxygen (O K α 1) at 0.540 KeV with 4.41 W%; 12.42 A%, Chlorine (Cl K α 1): at 2.6 KeV with 2.95 W%; 5.69 A% and potassium (K K α 1) at 3.35 KeV with 4.41 W%; 7.74 A%, and Carbon (C K α 1) at 0.277 KeV with 3.57 W%; 20.37 A%. The presence of Ag and O confirms the formation of the Ag₂O/Ag nanoparticles structure synthesis by the green method. This result agrees with [14-15].

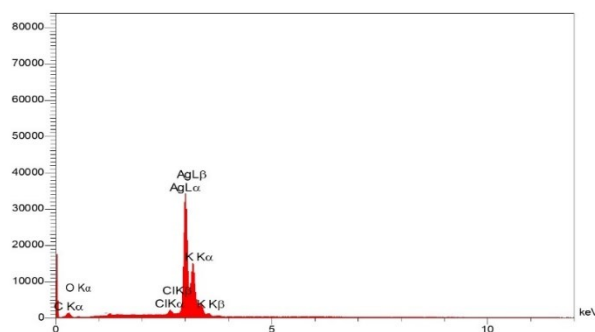
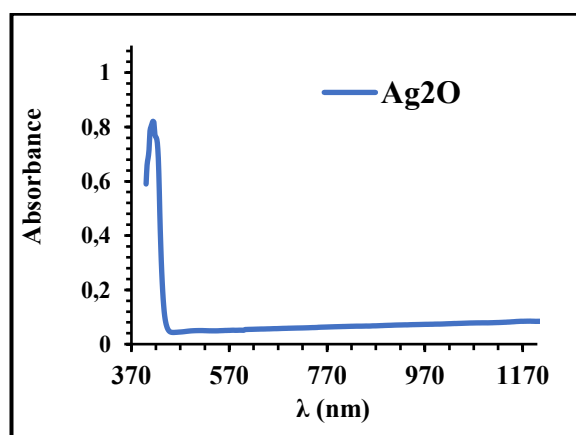


Figure 3. EDX spectrum of Ag₂O/Ag nanoparticles.

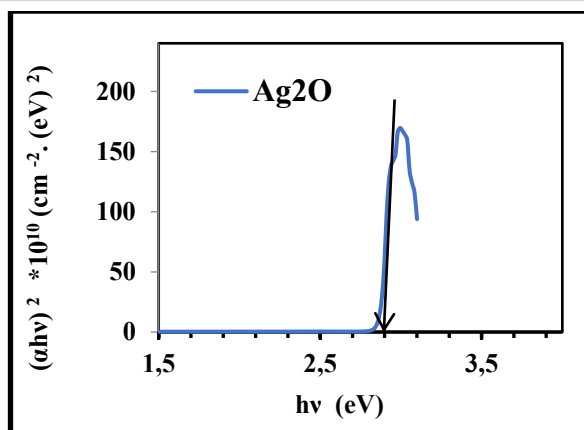
The optical properties of the Ag₂O/Ag nanoparticles were investigated using a UV-Vis spectrophotometer. The absorption spectrum with the wavelength range (190-1100 nm) of the electromagnetic spectrum and energy bandgap for the direct electronic transitions of the Ag₂O/Ag nanoparticles are shown in Fig. 4. The nanoparticles demonstrate nanocrystalline characteristics, Ag₂O/Ag displaying an absorption peak at 414 nm, falling in the violet region of the visible spectrum with a maximum absorbance of approximately 0.8. The absorbance decreases significantly right after its peak while maintaining a stable low value (below 0.2) throughout the visible and near-infrared spectrum from 570 to 1170 nm. The direct allowed energy bandgap (E_g) is accessed using Tauc's equation 3 by plotting $(\alpha h\nu)^2$ vs $h\nu$ via extrapolating a straight line on the energy axis [16].

$$\alpha h\nu = B (h\nu - E_g)^r \dots \dots \dots 3$$

Here: E_g is the energy gap between direct transitions, B is a constant dependent on the material type, $h\nu$ is photon energy, equal to $1240 \text{ eV} / \lambda$, and the power coefficient is symbolized by r ; The computation is based on potential electronic transitions, where a factor of $(1/2)$ represents direct allowed transitions, while $(3/2)$ represents a direct forbidden transition. The analysis of the curve using the indicated arrow demonstrates that the direct bandgap energy of Ag₂O/Ag nanoparticles approaches 2.88 eV. Traditionally observed in Ag₂O semiconductor nanostructures, the measured bandgap value matches the absorption edge from the UV-Vis spectrum. The Ag₂O/Ag nanoparticles would engage with incoming radiation through surface plasmon resonance because silver nanoparticles demonstrate powerful visible spectrum plasmonic responses. This result agrees with [17].



(a)



(b)

Figure 4. Optical properties (a) Uv-Vis absorption spectrum and (b) Energy bandgap (E_g) of $\text{Ag}_2\text{O}/\text{Ag}$ nanoparticles.

Fourier Transform Infrared Spectroscopy (FTIR) was used to investigate the functional groups and chemical bonds of the $\text{Ag}_2\text{O}/\text{Ag}$ nanoparticles. The FTIR spectra shown in Fig. 5 reveal significant functional groups. The FTIR spectrum of $\text{Ag}_2\text{O}/\text{Ag}$ nanoparticles shows multiple distinctive absorptions and functional groups across the wavenumber range of $4000\text{--}450\text{ cm}^{-1}$. The intense wide band located at 3430 cm^{-1} represents O-H stretching vibrations that stem from either surface hydroxyl groups or adsorbed water molecules. The infrared signal at 2873 before 2927 cm^{-1} arises from C-H vibrations. The band at 1632 cm^{-1} corresponds to the bending mode of water molecules that are bound to the surface. The C-O stretching vibrations likely produce two peaks at 1385 cm^{-1} and 1102 cm^{-1} . Ag-O bond vibrations appear in the wavenumber range below 1000 cm^{-1} while also being located around 515 cm^{-1} which validates the formation of Ag_2O nanoparticles. These functional groups verify the productive synthesis of $\text{Ag}_2\text{O}/\text{Ag}$ nanoparticles together with surface-adsorbed organic chemicals and water on the surface. This result agrees with [17-18].

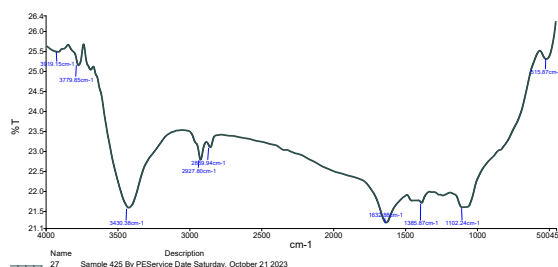


Figure 5. FTIR spectra of $\text{Ag}_2\text{O}/\text{Ag}$ nanoparticles.

Conclusion

The study presented *Hibiscus sabdariffa* extract successfully as an environmentally friendly reducing and stabilizing agent for the production of $\text{Ag}_2\text{O}/\text{Ag}$ nanoparticles using green synthesis. The extensive study confirmed the creation of cubic structured nanoparticles, which presented controlled dimensions in size. The XRD examination validated the crystal pattern and discovered crystallite elements with an average dimension of 35.60 nm through FESEM imaging, revealing irregular spherical shapes measuring 57.2 nm . The optoelectronic device applications are feasible because $\text{Ag}_2\text{O}/\text{Ag}$ nanoparticles exhibit a 2.88 eV bandgap combined with 414 nm absorption spectrum properties. The different functional groups evident in the FTIR spectra show that the nanoparticles received successful surface modification treatments. The environment-friendly production method of $\text{Ag}_2\text{O}/\text{Ag}$ nanoparticles becomes an encouraging pathway for large-scale industrial applications since it reduces environmental damage.

References

- [1] R. Kumar et al., “Application of Nanomaterials for Smart Devices,” *Nanotechnology: A Quick Guide to Materials and Technologies*, Bentham Science Publishers, pp. 1–25, 2024.
- [2] V. Girotra, P. Kaushik, and D. Vaya, “Exploring Sustainable Synthesis Paths: A Comprehensive Review of Environmentally Friendly Methods for Fabricating Nanomaterials Through Green Chemistry Approaches,” *Turkish Journal of Chemistry*, vol. 48, no. 5, pp. 703–725, 2024.
- [3] V. Girotra, P. Kaushik, and D. Vaya, “Exploring Sustainable Synthesis Paths: A Comprehensive Review of Environmentally Friendly Methods for Fabricating Nanomaterials Through Green Chemistry Approaches,” *Turkish Journal of Chemistry*, vol. 48, no. 5, pp. 703–725, 2024.
- [4] S. Yadav et al., “Biogenic Synthesis of Nanomaterials: Bioactive Compounds as Reducing and Capping Agents,” in *Biogenic Nanomaterials for Environmental Sustainability: Principles, Practices, and Opportunities*, Cham: Springer International Publishing, pp. 147–188, 2024.
- [5] N. Li, J. E. Simon, and Q. Wu, “Development of a Scalable, High-Anthocyanin and Low-Acidity Natural Red Food Colorant From *Hibiscus sabdariffa* L.,” *Food Chemistry*, vol. 461, p. 140782, 2024.
- [6] A. S. Gungure et al., “Studying the Properties of Green Synthesized Silver Oxide Nanoparticles in the Application of Organic Dye Degradation Under Visible Light,” *Scientific Reports*, vol. 14, no. 1, p. 26967, 2024.
- [7] J. O. Adeyemi et al., “Plant Extracts Mediated Metal-Based Nanoparticles: Synthesis and Biological Applications,” *Biomolecules*, vol. 12, no. 5, p. 627, 2022.
- [8] I. Kokina et al., “New Insights on Biosynthesis of Nanoparticles Using Plants Emphasizing the Use of Alfalfa (*Medicago sativa* L.),” *Journal of Nanotechnology*, vol. 2024, no. 1, p. 9721166, 2024.
- [9] T. Sarkar et al., “Structural, Spectroscopic and Morphology Studies on Green Synthesized ZnO Nanoparticles,” *Advances in Natural Sciences: Nanoscience and Nanotechnology*, vol. 14, no. 3, p. 035001, 2023.
- [10] A. Rasool et al., “Nature Inspired Nanomaterials, Advancements in Green Synthesis for Biological Sustainability,” *Inorganic Chemistry Communications*, vol. 2024, p. 112954, 2024.
- [11] F. Peng, J. Zhang, Z. Liu, X. Song, W. Zheng, and Y. Zeng, “A New Method for Calculating Interplanar Spacing to Distinguish Between Similar Phases in EBSD,” *Journal of Microscopy*, vol. 291, no. 2, pp. 186–196, 2023.
- [12] K. Mongkolsuttirat and J. Buajarern, “Uncertainty Evaluation of Crystallite Size Measurements of Nanoparticle Using X-Ray Diffraction Analysis (XRD),” in *Journal of Physics: Conference Series*, vol. 1882, p. 012054, 2021.
- [13] E. T. Salim et al., “Structural Morphological and Optical Investigations of Nano Silver Oxides Nanostructures,” *Key Engineering Materials*, vol. 936, pp. 73–82, 2022.
- [14] Ş. Altınsoy, K. Kızılbey, and H. B. İlim, “Green Synthesis of Ag and Cu Nanoparticles Using *Equisetum telmateia* Ehrh Extract: Coating, Characterization, and Bioactivity on PEEK Polymer Substrates,” *Materials*, vol. 17, no. 22, p. 5501, 2024.
- [15] H. A. Mohammed, M. J. Mohammed, and H. A. Ayesh, “Synthesis and Characterization of ZnO:Cu and Ag Bimetallics Nanoparticles by Sol–Gel Method,” *Nexo Revista Científica*, vol. 36, no. 06, pp. 1087–1102, 2023.
- [16] H. Zhong et al., “Idealizing Tauc Plot for Accurate Bandgap Determination of Semiconductor With Ultraviolet–Visible Spectroscopy: A Case Study for Cubic Boron Arsenide,” *Journal of Physical Chemistry Letters*, vol. 14, no. 29, pp. 6702–6708, 2023.
- [17] K. Kayed, M. Issa, and H. Al-Ourabi, “The FTIR Spectra of Ag/Ag₂O Composites Doped With Silver Nanoparticles,” *Journal of Experimental Nanoscience*, vol. 19, no. 1, p. 2336227, 2024.
- [18] I. M. Siddique, “Exploring Functional Groups and Molecular Structures: A Comprehensive Analysis Using FTIR Spectroscopy,” *Development*, vol. 1, p. 2, 2024.